Amplitude dependence of image quality in atomically-resolved bimodal atomic force microscopy

Hiroaki Ooe, Dominik Kirpal, Daniel S. Wastl, Alfred J. Weymouth, Toyoko Arai, and Franz J. Giessibl

Citation: Applied Physics Letters **109**, 141603 (2016); doi: 10.1063/1.4964125
View online: http://dx.doi.org/10.1063/1.4964125
View Table of Contents: http://scitation.aip.org/content/aip/journal/apl/109/14?ver=pdfcov
Published by the AIP Publishing

Amplitude dependence of image quality in atomically-resolved bimodal atomic force microscopy

Hiroaki Ooe,[1,2,a)] Dominik Kirpal,[1] Daniel S. Wastl,[1] Alfred J. Weymouth,[1] Toyoko Arai,[2] and Franz J. Giessibl[1]
[1]*Institute of Experimental and Applied Physics, University of Regensburg, D-93053 Regensburg, Germany*
[2]*Natural Science and Technology, Kanazawa University, Kanazawa, 920-1192 Ishikawa, Japan*

(Received 20 May 2016; accepted 21 September 2016; published online 5 October 2016)

In bimodal frequency modulation atomic force microscopy (FM-AFM), two flexural modes are excited simultaneously. We show atomically resolved images of KBr(100) in ambient conditions in both modes that display a strong correlation between the image quality and amplitude. We define the sum amplitude as the sum of the amplitudes of both modes. When the sum amplitude becomes larger than about 100 pm, the signal-to-noise ratio (SNR) drastically decreases. We propose that this is caused by the temporary presence of one or more water layers in the tip-sample gap. These water layers screen the short range interaction and must be displaced with each oscillation cycle. Decreasing the amplitude of either mode, however, increases the noise. Therefore, the highest SNR in ambient conditions is achieved when twice the sum amplitude is slightly less than the thickness of the primary hydration layer. *Published by AIP Publishing.* [http://dx.doi.org/10.1063/1.4964125]

Frequency modulation atomic force microscopy (FM-AFM)[1] is a powerful tool for investigating atomic-scale phenomena. The interaction between the tip, at the end of an oscillating cantilever, and the sample is measured via a change in the oscillation frequency of the cantilever. This frequency shift is a measure of the spatial derivative of the force in the direction of the tip oscillation. It has been shown that for FM-AFM measurements in vacuum, the maximum signal-to-noise ratio (SNR) is achieved with an oscillation amplitude slightly larger than the decay length of the signal of interest.[2] When investigating short range forces that decay at lengths comparable to interatomic distances, the highest SNR is achieved with amplitudes in the range from several tens of picometers to a few hundred picometers (small amplitudes).

Soft cantilevers that have a spring constant of $k < 100$ N/m (which is typical for commercial silicon cantilevers) require large amplitudes to prevent the tip from crashing into the surface at close distance (so-called "jump-to-contact").[3] For this reason, atomic resolution measurements with soft cantilevers require the use of large amplitudes from one nanometer to tens of nanometers.[4–6] One way to achieve controllable small amplitudes with soft cantilevers is to use a higher flexural mode which provides a much higher effective stiffness than the fundamental mode.[7] Theoretically, the effective stiffness of the second flexural mode is about 40 times higher than in the first flexural mode, and the resonance frequency is about 6.2 times higher.[8,9] This can be implemented with bimodal AFM,[10,11] in which the first flexural mode is excited at a large amplitude and the second flexural mode at a small amplitude to detect short range interactions.

Bimodal AFM has been used to obtain high-resolution results in ambient and vacuum environments.[11–13] It was shown that the small oscillation of the second flexural mode could be used to increase sensitivity to material properties.[14–17] Several groups have applied this technique to biological samples, including antibodies[13] and proteins.[11] Schwenk and coworkers used bimodal AFM to increase the contrast stemming from magnetic interaction with a ferromagnetic tip.[18,19] Kawai and coworkers explicitly demonstrated the advantage of a higher flexural mode oscillating at smaller amplitudes (amplitudes less than 100 pm) with a standard Si cantilever on a KBr(100) surface in UHV.[20] Moreno and coworkers achieved intramolecular resolution in UHV conditions at low temperature.[12] More recently, Santos and coworkers have started to consider the advantages of small oscillations in both flexural modes.[15,21]

In order to optimize the bimodal measurements for atomic resolution in both modes, data should be acquired with small amplitudes in both the first and second flexural modes.[15] This requires the use of a much stiffer sensor. In this Letter, we present data acquired with a qPlus sensor. The qPlus sensor is a self-sensing piezoelectric quartz cantilever with a large spring constant (here, $k = 1800$ N/m) that was originally built from a quartz tuning fork.[22,23] The high stiffness allows oscillation amplitudes of the first flexural mode smaller than one angstrom.[24,25] We collected data with two sensors equipped with a bulk sapphire tip. Sensor 1 had a free resonance frequency of the first mode $f_1 = 32\,596.7$ Hz, a quality factor of the first mode $Q_1 = 2906$, a free resonance frequency of the second mode $f_2 = 194\,858.2$ Hz and a quality factor of the second mode $Q_2 = 1848$. Sensor 2 had parameters $f_1 = 32\,858.6$ Hz, $Q_1 = 1944$, $f_2 = 196\,644.1$ Hz, and $Q_2 = 574$.

The amplitude of the first flexural mode, A_1 and of the second flexural mode, A_2, were independently set. These amplitudes were calibrated with a thermal spectrum and the ratio of the deflection sensitivity of two flexural modes.[8,23,26,27] The frequency shifts of the first flexural mode, Δf_1, and of the second flexural mode, Δf_2, were recorded in quasi-constant height mode using low gain integral feedback to compensate for thermal drift. This observation mode was chosen to show the short-range force contribution to Δf_1 and Δf_2 independently. If we had used the topographic mode controlling on Δf_1 as demonstrated previously in Ref. 24, any atomic contrast

a)Electric mail: hiroakiooe@se.kanazawa-u.ac.jp

in the Δf_2 channel would not necessarily originate from short range forces. Only the use of the constant-height mode allows to simultaneously assess the atomic contrast contributions of Δf_1 and Δf_2.

We performed measurements in ambient conditions on KBr(100). In our laboratory, the relative humidity (RH) varies from 40% to 70% throughout the year. A XPS study by Arima and coworkers showed the KBr surface to be covered by adsorbed water at ~30% RH and the thickness of the water layer to remain constant up to 60% RH. At higher humidity, the thickness increased only slightly from 60% to 85% RH and rapidly increased above 85% RH.[28] More important to AFM studies, however, is the capillary action of the water, which causes a much thicker water layer at the tip-sample interface (e.g., Ref. 29), on the order of tens of nanometers. The capillary action is indeed a function of the relative humidity but also a function of the geometry of the mesoscopic tip apex (see e.g., Ref. 30) which is inaccessible to us. Therefore all data reported in this Letter is collected with the tip apex inside the layer of adsorbed water. That is, the tip does not leave and re-penetrate into this water layer within a cycle.

Within the water layer, near polar surfaces, water molecules order and form hydration layers with a thickness of ~200 to 310 pm.[24,25,31–37] In the previous work, the ideal amplitude of oscillation was determined for single-mode FM-AFM measurements in ambient conditions.[24,25,31] On the KBr(100) surface, the highest SNR was observed with an amplitude of $A \sim 75$ pm.[24] With smaller amplitudes, the signal becomes noisier due to instrumental noise.[1,27,38] With larger amplitudes, the SNR suffers for two reasons: The average tip-sample distance becomes larger, reducing the signal, and water molecules come between the tip and sample. The tip needs to penetrate the hydration layer during each oscillation cycle and the water molecules screen the short-range interaction.[24] Because of these effects, the SNR is enhanced when the peak-to-peak amplitude is slightly smaller than the thickness of a single ordered hydration layer.[25]

Images of KBr taken with sensor 1 are shown in Figure 1. The oscillation models of the first and second flexural modes are shown in Figures 1(a) and 1(b). First we collected single-mode images, exciting either the first or the second flexural mode at $A = 75$ pm. This is the optimal amplitude for single-mode measurements as determined in Ref. 24. Figure 1(c) is a Δf_1 image taken with only the first flexural mode excited at $A_1 = 75$ pm, and Figure 1(d) is a Δf_2 image taken with only the second flexural mode excited at $A_2 = 75$ pm. Atomic resolution can clearly be seen in both images. We then investigated if the two modes influence each other. To do this, we first acquired Δf_1 data with only the first flexural mode excited, then also excited the second mode. Figures 1(e) and 1(f) show simultaneously acquired Δf_1 and Δf_2. The slow scan direction of these imaging was downward. Down to line A, only the first flexural mode was excited at $A_1 = 75$ pm, and the atomic resolution can be clearly seen in Δf_1. From line A down, the second flexural mode is also excited at $A_2 = 75$ pm, and the Δf_2 controller was turned on from line B. With both modes excited, the Δf_1 image becomes much weaker. We note that these images are line flattened for clarity. The raw image and simultaneously obtained topography (Z) images are shown in Fig. S1 (see supplementary material).

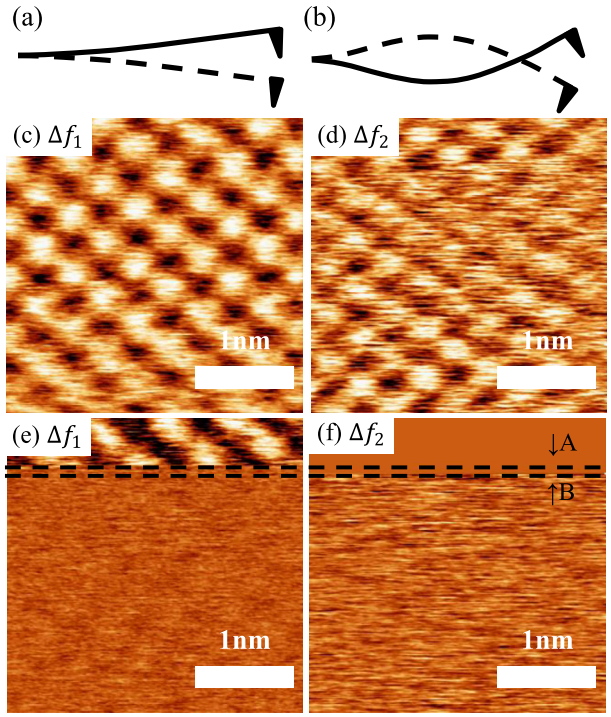

FIG. 1. Schematics of (a) first and (b) second flexural mode. (c) Δf_1 image with only the first flexural mode excited at $A_1 = 75$ pm. (d) Δf_2 with only the second flexural mode excited at $A_2 = 75$ pm. (e) Δf_1 and (f) Δf_2 images simultaneously acquired. Up to line A, only the first mode was excited at $A_1 = 75$ pm. Past line B, both modes were excited at $A_1 = A_2 = 75$ pm. The scan area is 3 × 3 nm^2 and the scan speed is 58 nm/s. For clarity, all images were line-flattened, the frequency shift ranges from 164 to 352 Hz in (c) and from 166 to 220 Hz in (d). Raw data are available online (supplementary material).

Initially, this result was rather surprising to us. Mathematically, the first and second flexural modes of a cantilever are orthogonal, and we would not expect them to influence each other. Addition of the second flexural mode does not strongly affect the average position of the cantilever during the period of the first mode. We therefore acquired further data with both modes at various amplitudes.

Figure 2 shows images of Δf_1 and Δf_2 with both flexural modes excited at amplitudes of 75 pm, 53 pm, and 40 pm. When $A_1 = A_2 = 75$ pm, the (a) Δf_1 image and (b) Δf_2 image show faint atomic contrast similar to that in Figure 1(e). The images improve when the amplitudes are decreased, as can be seen in Figures 2(c) and 2(d), for which $A_1 = A_2 = 53$ pm. Very clear images are obtained when $A_1 = A_2 = 40$ pm, shown in Figures 2(e) and 2(f). These results imply that, in the case of bimodal FM-AFM, the SNR is maximized when both amplitudes are similar to half of the optimal amplitude for single-mode. We therefore define the sum amplitude as the sum of the amplitudes of both flexural modes: $A_{\mathrm{sum}} = 2\,(A_1 + A_2)$. In order to quantitatively validate the amplitude dependence of the SNR, we repeated measurements with the two different sensors and analyzed the SNR from multiple images.

To determine the SNR, we took a Fourier transform of the data and compared the height of the peak corresponding to the atomic signal with the background noise. Figure 2(g) is a plot of the SNR of Δf_1 as a function of the sum amplitude.

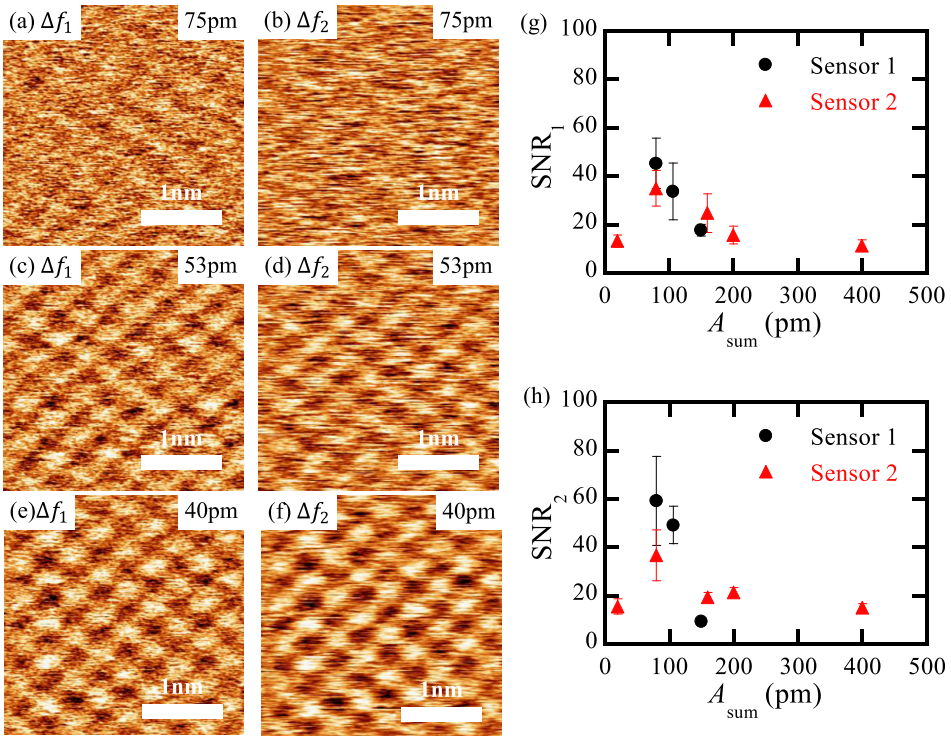

FIG. 2. Bimodal FM-AFM images taken in which $A_1 = A_2$. (a and b) $A_1 = A_2 = 75$ pm (c and d) $A_1 = A_2 = 53$ pm (e and f) $A_1 = A_2 = 40$ pm. The SNR of (g) Δf_1 and (h) Δf_2 as the function of A_{sum}. Error bars correspond to standard deviations of each SNR. Collectively 116 images were used for this analysis as 30 pairs of Δf_1 and Δf_2 images were collected with sensor 1 and 28 pairs with sensor 2. The scan area is $3 \times 3\,nm^2$ and the scanning speed is 58 nm/s. Images are line-flattened for clarity, the frequency shift ranges are 57–140 Hz in (a), 21–37 Hz in (b), 107–195 Hz in (c), 39–61 Hz in (d), 460–612 Hz in (e) and 122–161 Hz in (f). Raw data are available online (supplementary material).

Figure 2(h) is a plot of the SNR of Δf_2 as a function of the sum amplitude. Both plots show the highest SNR, for both sensors, around $A_{sum} \sim 80$ pm. The Δf images taken with sensor 2 and a more detailed description of the SNR analysis are given in Figs. S4 and S5 (see supplementary material).

Similar to previous findings in vacuum,[2] we find an optimal SNR for amplitudes less than an Angstrom. However, empirically we find a notable difference to the decrease of SNR when increasing the amplitude beyond its optimal value A_{opt}. In vacuum, SNR decreases at a relatively small rate of approximately $(A_{opt}/A)^{0.5}$.[2] In ambient environments with a liquid adsorption layer, we find a much stronger decay of image quality with sum amplitude as shown in Figs. S5(a) and S5(d) (see supplementary material). The vertical range that is covered by the oscillating cantilever is twice the sum amplitude. We propose that using sum amplitudes greater than half the thickness of the first hydration layer (approx. 200 pm) allows water molecules to penetrate the gap between the tip apex and the sample, reducing the image quality.

We then varied A_1 and A_2, keeping A_{sum} approximately constant at the optimal value of ~80 pm, as determined above. In Figures 3(a) and 3(b), $A_1 = 60$ pm and $A_2 = 15$ pm. Atomic contrast can be seen in both Δf_1 and Δf_2, but Δf_1 shows higher SNR. In Figures 3(c) and 3(d), $A_1 = A_2 = 40$ pm and the SNR

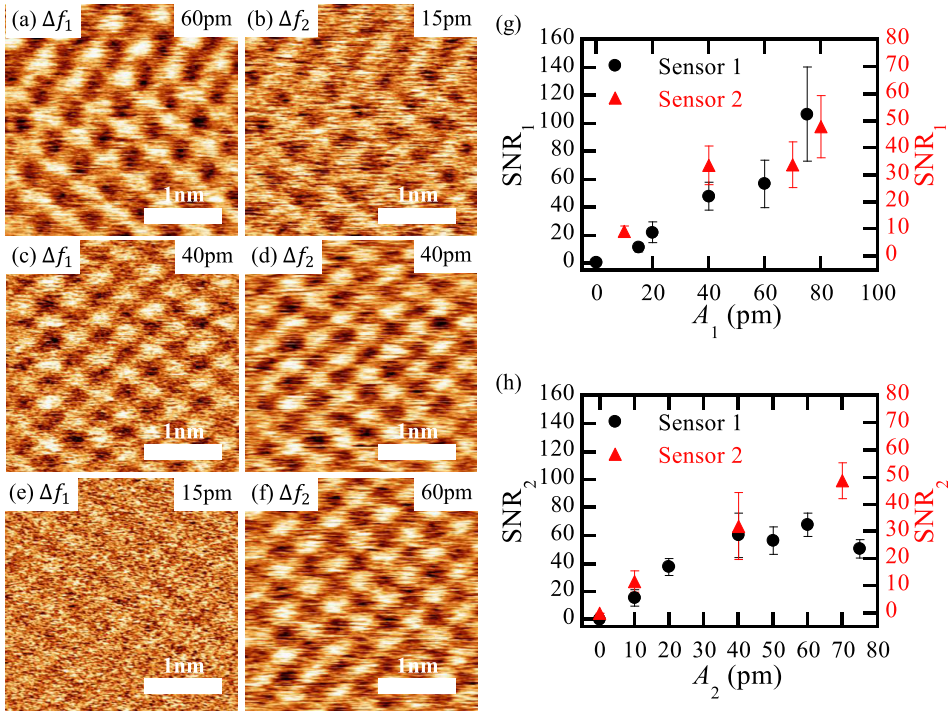

FIG. 3. A survey of images taken with different A_1 and A_2 values for $A_1 + A_2 \sim 80$ pm. (a) Δf_1 image with $A_1 = 60$ pm, and (b) Δf_2 image with $A_2 = 15$ pm. (c) Δf_1 image with $A_1 = 40$ pm, and (d) Δf_2 image with $A_2 = 40$ pm. (e) Δf_1 image with $A_1 = 15$ pm, and (f) Δf_2 image with $A_2 = 60$ pm. The SNR of (g) Δf_1 and (h) Δf_2 as the function of A_{sum}. Error bar corresponds to standard deviations of each SNR. Collectively, 220 images are used for this analysis as 64 pairs of Δf_1 and Δf_2 images collected sensor 1 and 46 pairs with sensor 2. The scan area is $3 \times 3\,nm^2$ and the scan speed is 58 nm/s. Images are line-flattened for clarity, the frequency shift ranges are 166–281 Hz in (a), 40–71 Hz in (b), 460–612 Hz in (c), 122–161 Hz in (d), 217–420 Hz in (e) and 70–91 Hz in (f). Raw data are available online (supplementary material).

of the two images are similar. Finally, in Figures 3(e) and 3(f), $A_1 = 15\,\text{pm} < A_2 = 60\,\text{pm}$, and the corresponding Δf_2 image has a higher SNR. These results show that the SNR of each mode is individually controllable and is higher with larger amplitudes. Instrumental noise decreases with increasing amplitude. For each mode individually, larger amplitudes correspond to lower overall noise, as expected when considering the noise contributions in FM-AFM.[1,27,38] Similar to the SNR analysis for the data presented in Figs. 2(g) and 2(h), we performed a similar analysis to about 100 images collected with two different tips. Figures 3(g) and 3(h) show the plot of the SNR of Δf_1 and Δf_2 vs. each amplitudes of that flexural mode. These plots show a monotonic increase of SNR as the amplitude of that flexural mode increases when A_{sum} is less than half of the thickness of single hydration layer (supplementary material).

In vacuum, the optimal amplitude is given by the balance between less noise at larger amplitudes at the cost of a smaller signal for larger amplitudes, resulting in an optimal amplitude that is approximately given by the decay length of the short-range interaction.[2] In ambient conditions, the noise in frequency measurements also decreases for larger amplitudes, but the frequency shift signal induced by short-range interactions drops rapidly once the motion of the tip is large enough to admit water molecules in the tip-sample gap. The result is that the ideal amplitudes for bimodal FM-AFM follow the same pattern as for single-mode FM-AFM measurements. In ambient conditions, the sum amplitude must be smaller than the thickness of a hydration layer to ensure that the tip does not leave and re-penetrate into a hydration layer with each cycle. At the same time, the amplitude has to be as large as possible to reduce the noise. The resolution, which is proportional to SNR, of each mode can be increased by increasing its amplitude up to the ideal sum amplitude.

In this study, we investigated the effect of the amplitude of the first and second flexural modes on the image quality of bimodal FM-AFM measurements with small amplitudes in ambient conditions. Two orthogonal flexural modes can have a strong influence on each other. This is due to the hydration layer on the sample surface. We showed that for this system, maximizing the SNR for both Δf_1 and Δf_2 results in the requirement that $A_1 = A_2$. Our results show that conventional bimodal AFM would benefit from stiffer cantilevers that enable atomic resolution in both frequency shift channels.

See supplementary material for the topography (Z) and raw Δf images of the figures in the main text, the images collected with different sensor, all SNR data and a detailed explanation of the SNR derivation.

Funding was provided by Deutsche Forschungsgemeinschaft under GRK 1570 and by "Strategic Young Researcher Overseas Visits Program for Accelerating Brain Circulation" from the Japan Society for the Promotion of Science. The authors gratefully acknowledge the support for this study provided by Kanazawa University SAKIGAKE Project.

[1]T. R. Albrecht, P. Grütter, D. Horne, and D. Rugar, J. Appl. Phys. **69**, 668 (1991).
[2]F. J. Giessibl, H. Bielefeldt, S. Hembacher, and J. Mannhart, Appl. Surf. Sci. **140**, 352 (1999).
[3]F. J. Giessibl, Phys. Rev. B **56**, 16010 (1997).
[4]F. J. Giessibl, Science **267**, 68 (1995).
[5]S. Kitamura and M. Iwatsuki, Jpn. J. Appl. Phys. **34**, L145 (1995).
[6]K. Fukui, H. Onishi, and Y. Iwasawa, Phys. Rev. Lett. **79**, 4202 (1997).
[7]S. Kawai, S. Kitamura, D. Kobayashi, S. Meguro, and H. Kawakatsu, Appl. Phys. Lett. **86**, 193107 (2005).
[8]S. Rast, C. Wattinger, U. Gysin, and E. Meyer, Rev. Sci. Instrum. **71**, 2772 (2000).
[9]R. C. Tung, T. Wutscher, D. Martinez-Martin, R. G. Reifenberger, F. J. Giessibl, and A. Raman, J. Appl. Phys. **107**, 104508 (2010).
[10]T. R. Rodriguez and R. Garcia, Appl. Phys. Lett. **84**, 449 (2004).
[11]R. Garcia and E. T. Herruzo, Nat. Nanotechnol. **7**, 217 (2012).
[12]C. Moreno, O. Stetsovych, T. K. Shimizu, and O. Custance, Nano Lett. **15**, 2257 (2015).
[13]N. F. Martinez, J. R. Lozano, E. T. Herruzo, F. Garcia, C. Richter, T. Sulzbach, and R. Garcia, Nanotechnology **19**, 384011 (2008).
[14]N. F. Martinez, S. Patil, J. R. Lozano, and R. Garcia, Appl. Phys. Lett. **89**, 153115 (2006).
[15]S. Santos, Appl. Phys. Lett. **103**, 231603 (2013).
[16]S. D. Solares and G. Chawla, J. Appl. Phys. **108**, 054901 (2010).
[17]G. Chawla and S. D. Solares, Appl. Phys. Lett. **99**, 074103 (2011).
[18]J. Schwenk, M. Marioni, S. Romer, N. R. Joshi, and H. J. Hug, Appl. Phys. Lett. **104**, 112412 (2014).
[19]J. Schwenk, X. Zhao, M. Baconi, M. A. Manioni, S. Romer, and H. J. Hug, Appl. Phys. Lett. **107**, 132407 (2015).
[20]S. Kawai, T. Glatzel, S. Koch, B. Such, A. Baratoff, and E. Meyer, Phys. Rev. Lett. **103**, 220801 (2009).
[21]S. Santos, V. Barcons, H. K. Christenson, D. J. Billingsley, W. A. Bonass, J. Font, and N. H. Thomson, Appl. Phys. Lett. **103**, 063702 (2013).
[22]F. J. Giessibl, Appl. Phys. Lett. **73**, 3956 (1998).
[23]F. J. Giessibl, Appl. Phys. Lett. **76**, 1470 (2000).
[24]D. S. Wastl, A. J. Weymouth, and F. J. Giessibl, Phys. Rev. B **87**, 245415 (2013).
[25]D. S. Wastl, A. J. Weymouth, and F. J. Giessibl, ACS Nano **8**, 5233 (2014).
[26]J. Welker, F. F. Elsner, and F. J. Giessibl, Appl. Phys. Lett. **99**, 084102 (2011).
[27]F. J. Giessibl, Rev. Mod. Phys. **75**, 949 (2003).
[28]K. Arima, P. Jiang, X. Deng, H. Bluhm, and M. Salmeron, J. Phys. Chem. C **114**, 14900 (2010).
[29]A. L. Weisenhorn, P. K. Hansma, T. R. Albrecht, and C. F. Quate, Appl. Phys. Lett. **54**, 2651 (1989).
[30]D. L. Sedin and K. L. Rowlen, Anal. Chem. **72**, 2183 (2000).
[31]D. S. Wastl, M. Judmann, A. J. Weymouth, and F. J. Giessibl, ACS Nano **9**, 3858 (2015).
[32]M. Luna, F. Rieutord, N. A. Melman, Q. Dai, and M. Salmeron, J. Phys. Chem. A **102**, 6793 (1998).
[33]S. Jeffery, P. M. Hoffmann, J. B. Pethica, C. Ramanujan, H. Ozgur Ozer, and A. Oral, Phys. Rev. B **70**, 054114 (2004).
[34]T. Fukuma, M. J. Higgins, and S. P. Jarvis, Biophys. J. **92**, 3603 (2007).
[35]K. Kimura, S. Ido, N. Oyabu, K. Kobayashi, and Y. Hirata, J. Chem. Phys. **132**, 194705 (2010).
[36]J. N. Israelachvili and R. M. Pashley, Nature (London) **306**, 249 (1983).
[37]J. I. Kilpatrick, S. Loh, and S. P. Jarvis, J. Am. Chem. Soc. **135**, 2628 (2013).
[38]K. Kobayashi, H. Yamada, and K. Matsushige, Rev. Sci. Instrum. **82**, 033702 (2011).